RESEARCH ARTICLE | JULY 06 2020

Active dopant profiling and Ohmic contacts behavior in degenerate n-type implanted silicon carbide

Monia Spera; Giuseppe Greco ; Andrea Severino; Marilena Vivona ; Patrick Fiorenza ; Filippo Giannazzo ; Fabrizio Roccaforte

Appl. Phys. Lett. 117, 013502 (2020)
https://doi.org/10.1063/5.0012029

Applied Physics Letters ARTICLE scitation.org/journal/apl

Active dopant profiling and Ohmic contacts behavior in degenerate n-type implanted silicon carbide

Cite as: Appl. Phys. Lett. **117**, 013502 (2020); doi: 10.1063/5.0012029
Submitted: 28 April 2020 · Accepted: 22 June 2020 ·
Published Online: 6 July 2020

Monia Spera,[1] Giuseppe Greco,[1] Andrea Severino,[2] Marilena Vivona,[1] Patrick Fiorenza,[1] Filippo Giannazzo,[1] and Fabrizio Roccaforte[1,a)]

AFFILIATIONS

[1]Consiglio Nazionale delle Ricerche – Istituto per la Microelettronica e Microsistemi (CNR-IMM), Strada VIII, n. 5 Zona Industriale, 95121 Catania, Italy
[2]STMicroelectronics, Stradale Primosole 50, 95121 Catania, Italy

[a)]**Author to whom correspondence should be addressed**: fabrizio.roccaforte@imm.cnr.it

ABSTRACT

This Letter reports on the active dopant profiling and Ohmic contact behavior in degenerate P-implanted silicon carbide (4H-SiC) layers. Hall measurements showed a nearly temperature-independent electron density, corresponding to an electrical activation of about 80% of the total implanted dose. Using the Hall result as calibration, the depth resolved active P-profile was extracted by scanning capacitance microscopy (SCM). Such information on the active P-profile permitted to elucidate the current injection mechanism at the interface of annealed Ni Ohmic contacts with the degenerate n-type 4H-SiC layer. Modeling the temperature dependence of the specific contact resistance with the thermionic field emission mechanism allowed extracting a doping concentration of $8.5 \times 10^{19}\,cm^{-3}$ below the metal/4H-SiC interface, in excellent agreement with the value independently obtained by the SCM depth profiling. The demonstrated active dopant profiling methodology can have important implications in the 4H-SiC device technology.

Owing to its superior properties, silicon carbide (4H-SiC) is an excellent candidate to replace silicon devices,[1] obtaining a better energy efficiency in high-temperature, high-power, and high-frequency applications.[2,3] Because of the low diffusivity of the dopant species in SiC, ion-implantation is the method of choice for selective area doping in the fabrication of devices, such as Schottky diodes, metal oxide semiconductor field effect transistors (MOSFETs), and junction barrier Schottky (JBS) diodes.[1,4] N-type regions are usually formed by nitrogen (N) or phosphorus (P) ion-implantation, while aluminum (Al) is used as the p-type dopant. After implantation, annealings at very high temperatures (>1500 °C) are necessary for the electrical activation of the dopants.

Understanding and controlling the ion-implantation doping in 4H-SiC is extremely important because the implanted regions are crucial parts of the devices. In particular, high concentration ($>10^{20}\,cm^{-3}$) Al- or P-implanted regions are present in both JBS diodes and MOSFETs to minimize the resistance of Ohmic contacts on the p- or n-type regions.

Hall-effect measurements represent the standard method to evaluate the carrier density and mobility in high-dose implanted 4H-SiC layers. In the case of Al-implanted 4H-SiC layers, the activation energy and the active fraction of the p-type Al-dopants are evaluated from the temperature dependence of the hole density applying the neutrality equation.[5,6] For the n^+-type 4H-SiC layers, the neutrality equation has been successfully applied to evaluate the electrical activation only for P-concentrations up to $10^{19}\,cm^{-3}$.[7] On the other hand, higher P-concentrations result in a degenerate semiconductor.[8–12] Since the substitutional P-fraction cannot be inferred from the neutrality equation in degenerate semiconductors, the common approach to evaluate the electrical activation is to calculate the ratio of the electron concentration from Hall measurements with respect to the overall P-implanted dose. As an example, for the P-concentration of $1 \times 10^{20}\,cm^{-3}$, an electrical activation of more than 70% was measured,[9,12] while an almost complete activation was estimated for a dose of $2 \times 10^{20}\,cm^{-3}$.[11]

While Hall-effect measurements provide an average value of the carrier concentration over the implanted thickness, for many applications, a depth resolved information on the dopant concentration is desired. For this purpose, in the past decades, carrier profiling

methods, such as scanning capacitance microscopy (SCM) and scanning spreading resistance microscopy (SSRM), have been employed in the n- and p-type implanted 4H-SiC.[13–16] In particular, the SCM technique, based on differential capacitance measurements, is able to provide direct information on the active dopant concentration in 4H-SiC.[13,14] On the other hand, the SSRM technique, based on resistance measurements, is sensitive to the resistivity profile in the implanted 4H-SiC, which is related to both the carrier concentration and the mobility.[15] However, quantitative active dopant profiling in the degenerate n-type doped 4H-SiC has not been reported so far, as dedicated calibration procedures must be developed for this purpose.

In this Letter, the active dopant profiling and the Ohmic contact behavior in high P concentration ($\approx 1 \times 10^{20}\,cm^{-3}$) 4H-SiC implanted layers have been elucidated by the combination of integral carrier density measurement by the Hall-effect and SCM depth carrier profiling.

4H-SiC wafers with an n-type epitaxy ($1 \times 10^{16}\,cm^{-3}$ nitrogen doping) were the starting materials for these experiments. A p-type Al-implantation doping on the order of $1 \times 10^{17}\,cm^{-3}$ was performed before the high concentration P-implants, to achieve a vertical isolation of the n^+ implanted layer. In this way, parallel conduction effects during electrical measurements are prevented, as the current flows in the highly conductive n^+ implanted layer. The P-implants were carried out at a temperature of 400 °C using multiple energies (from 30 to 200 keV) and ion doses (7.5×10^{13}–$5 \times 10^{14}\,cm^{-2}$). The post-implantation annealing at 1675 °C was performed in Ar ambient, with the wafer surface coated by a carbon capping layer.[17] After annealing, the carbon capping layer was removed with an oxidation process.[17] Then, the depth profile of the implanted P was measured by secondary-ion mass spectrometry (SIMS). Therefore, Van der Pauw (VdP) and Transmission Line Model (TLM) test patterns were fabricated to evaluate the electrical properties of the implanted layer. The VdP test patterns were fabricated by creating isolated n-type implanted square structures with Ni_2Si Ohmic contacts at the four corners, defined by lithography, lift-off, and annealing at 950 °C of 100 nm Ni films.[18] These contacts were small with respect to the entire sample size, thus allowing using the classical VdP formula without correction factors for the analysis of the electrical data.[19] Sheet resistance and Hall-effect measurements on these structures were carried out using a variable temperature Hall-effect measurement system from MMR Technologies. To determine the specific contact resistance (ρ_c), TLM structures were fabricated by defining Ni_2Si contacts placed at different distances and were laterally isolated by trench etching.[19] The current–voltage (I–V) measurements on the TLM structures were performed in a Karl Suss Microtec probe station equipped with a HP 4156B parameter analyzer, in a four-point probe configuration. Active phosphorous profiling by SCM was carried out on a 4H-SiC wafer with the n-type epitaxy directly implanted with P, i.e., without the p-type vertical isolation implant. The samples were cross-sectioned using the procedure described in Ref. 14, and analyses were performed with a DI 3100 microscope with a Nanoscope V controller.

Figure 1 reports a comparison of the experimental chemical P-profile determined by SIMS analysis with the profile simulated using the SRIM code (The Stopping and Range of Ions in Matter).[20] As can be seen, a good agreement between the experimental data and the simulation is obtained, except for the discrepancy observed at larger depths (above 250 nm), which is due to channeling effects occurring during the implantation of 4H-SiC.[4]

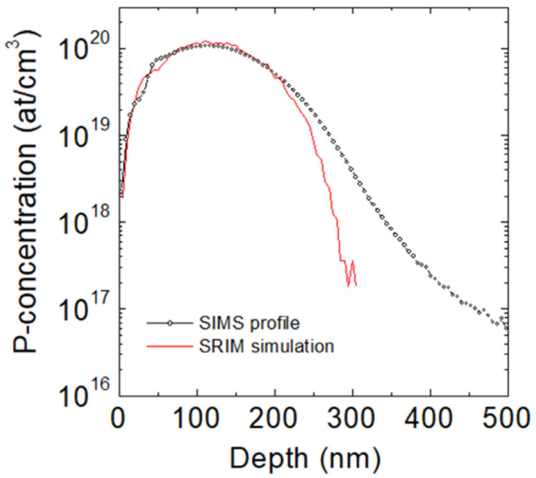

FIG. 1. Comparison of the experimental chemical P-profile obtained by SIMS with the SRIM simulated profile.

Then, VdP and Hall-effect measurements were carried out from 300 to 500 K to investigate the temperature dependence of the sheet resistance and the carrier density, which determine the carrier transport in this high P-concentration implanted layer. Since the nominal dopant level of the n^+ implanted layer is on the order of $10^{20}\,cm^{-3}$, the contribution of minority carrier (holes) conductivity is negligible and Hall-effect measurements give information on the electron concentration.

Figure 2 shows the temperature dependence of the sheet resistance R_{SH} (a) and of the electron density n (b). At room temperature, the implanted layer has a sheet resistance of $R_{SH} = 181\ \Omega$/sq and an electron density of $n = 1.44 \times 10^{15}\,cm^{-2}$. While R_{SH} exhibits a slight increase from 181 to 212 Ω/sq with increasing the measurement temperature from 300 to 500 K [Fig. 2(a)], the electron density remains nearly constant in the same temperature range [Fig. 2(b)]. Such a behavior is typically observed in degenerate semiconductors.[8,9]

The insets of Fig. 2 report the behavior of p-type 4H-SiC layers implanted with Al at similar dose and subjected to the same annealing

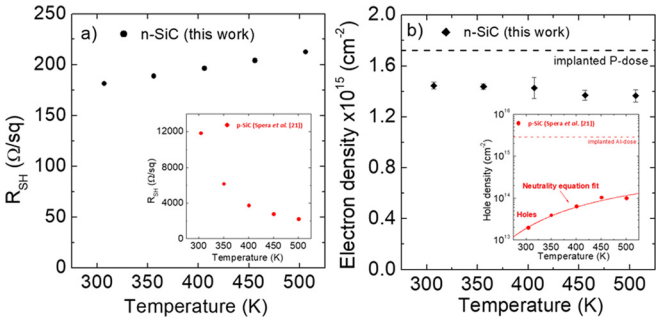

FIG. 2. Temperature-dependence of the sheet resistance R_{SH} (a) and the electron density (b) in the P-implanted 4H-SiC. The insets show the results obtained on the p-type 4H-SiC layers implanted with Al at an equivalent dose and annealed under the same conditions.[21] The insets are adapted with permission from Spera *et al.*, Mater. Sci. Semicond. Process. **93**, 274–279 (2019).[21] Copyright 2019 Elsevier Ltd.

temperature.[21] As can be seen, in the case of the p-type doped 4H-SiC, the sheet resistance strongly decreases with the temperature, while the hole concentration increases. This different behavior is due to the high ionization energy of the p-type dopant specie (Al) with respect to the n-type one (P).[7,22] Hence, the electrically active fraction of the p-type Al dopant and the compensation can be evaluated by fitting the temperature-dependent Hall density with the neutrality equation, as described in Refs. 21 and 23.

Fujhiara *et al.*[7] used the neutrality equation to analyze the behavior of the n-type 4H-SiC samples implanted with lower P concentrations (in the range of 10^{17}–10^{19} cm^{-3}) and estimated an electrical activation of about 98%.

However, in the present case of the n^+-type ($\sim 10^{20}$ cm^{-3}) P-implanted 4H-SiC layer, the neutrality equation cannot be applied since the electron density is almost independent of the temperature. Under these degenerate doping conditions, the donor energy level broadens and merges with the 4H-SiC conduction band. Therefore, it is reasonable to assume that most of the P donors (occupying a substitutional position in the 4H-SiC lattice) are ionized. Hence, the ratio between the electron density from Hall measurements and the P-dose from SIMS measurements can be taken as the lower limit to the electrical activation. In our case, a peak concentration of $\sim 1 \times 10^{20}$ cm^{-3} at a depth of ~100 nm and a total implanted dose of 1.72×10^{15} cm^{-2} can be determined from the SIMS profile (see Fig. 3). Hence, an electrical activation of more than 80% of the implanted P-ions can be deduced.

Achieving a high electrical activation represents a prerequisite for fabricating low resistance Ohmic contacts on the n-type 4H-SiC. However, the determination of the depth distribution of the electrically active dopant in the implanted region, and, specifically, the concentration value at the interface with the metal, is essential to quantitatively describe the mechanisms of electronic transport at the metal/4H-SiC interface.

Hence, the n-type implanted 4H-SiC layer has been studied by means of SCM on a cross-sectioned sample. The quantification of the SCM raw data (dC/dV) into an electrically active P-profile was obtained by normalizing the area under the SCM profile to the electron dose evaluated by Hall measurements. Figure 3 shows the comparison of the electrically active P-concentration profile by SCM with the SIMS chemical profile. Noteworthy, the SCM profile is nearly coincident with the SIMS profile in the surface region and in the tail of the P implant, whereas it exhibits a plateau of $\sim(8.5–9) \times 10^{19}$ cm^{-3} in the depth range from 70 to 160 nm. The lower concentration level in this plateau region and the slight differences in the width of the two profiles can be ascribed to the presence of implantation-induced defects, leading to an incomplete activation of implanted P.

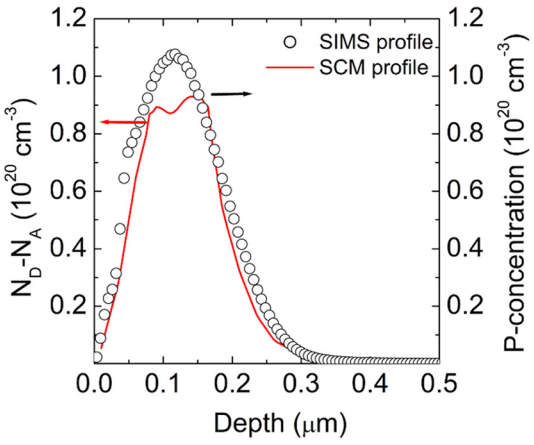

FIG. 3. Electrically active P-profile obtained by SCM (left scale) and chemical P-profile by SIMS (right scale). The SCM profile has been normalized considering the electron density determined by Hall-effect measurements as the calibration.

This depth resolved distribution of the active dopant concentration determined by SCM is important to shed light on the mechanism of the current injection in nickel silicide (Ni_2Si) Ohmic contacts on the highly n-type doped 4H-SiC, which represent the standard source-contacts in power MOSFETs. The formation of Ni_2Si Ohmic contacts upon annealing at 950 °C of the Ni film causes the consumption of the 4H-SiC material and the recession of the Ni_2Si/4H-SiC interface below the original surface. During reaction, carbon clusters are uniformly distributed inside the silicide layer, with a slight accumulation a few nanometers far away from the interface with SiC.[18]

Considering the reaction associated with the Ni_2Si formation ($SiC + 2Ni \rightarrow Ni_2Si + C$), the molar amount of Ni consumed by this reaction is double with respect to that of SiC ($n_{Ni} = 2n_{SiC}$). Then, considering that $\rho_{SiC} = 3.21$ g/cm^3 and $\rho_{Ni} = 8.9$ g/cm^3 are, respectively, the density of SiC and Ni, and $M_{SiC} = 40.11$ g/mol and $M_{Ni} = 58.7$ g/mol are the molar weights for SiC and Ni, the thickness ratio between the original Ni layer (t_{Ni}) and the consumed SiC layer (t_{SiC}) is given by[24]

$$\frac{t_{SiC}}{t_{Ni}} = \frac{1}{2}\frac{\rho_{Ni}}{M_{Ni}}\left(\frac{\rho_{SiC}}{M_{SiC}}\right)^{-1} = 0.95, \quad (1)$$

where $\frac{\rho_{Ni}}{M_{Ni}}$ and $\frac{\rho_{SiC}}{M_{SiC}}$ give the atomic density of Ni and SiC, respectively.

Considering the 100 nm Ni films used in our experiment, a consumption of about 95 nm of SiC has been estimated, thus indicating the depth of the Ni_2Si/4H-SiC interface.

While the SCM analysis permits evaluating the electrically active P-profile throughout the implanted layer, the study of the current transport mechanism at the metal/semiconductor interface by means of TLM patterns gives information about the doping at the interface created after the silicide formation. For this aim, the electrical behavior of the nickel silicide Ohmic contact on the degenerate n-type doped 4H-SiC layer has been studied.

First, TLM measurements at room temperature gave a specific contact resistance of $\rho_c = 5.4 \times 10^{-6}\ \Omega \cdot \text{cm}^2$ and a sheet resistance of $R_{SH} = 180\ \Omega$/sq.

Then, the specific contact resistance ρ_c has been monitored as a function of the measurement temperature T, between 300 K and 400 K. Figure 4 reports the temperature-dependence of ρ_c, where the ρ_c values decrease with the increase in the measurement temperature. The study of the current transport mechanism permits the evaluation of the donor concentration at the metal/4H-SiC interface. A useful parameter to determine which current transport mechanism is predominant through the contact is the characteristic energy E_{00}, related to the doping concentration N_D according to

$$E_{00} = \frac{qh}{4\pi}\sqrt{\frac{N_D}{\varepsilon_S m^*}}, \quad (2)$$

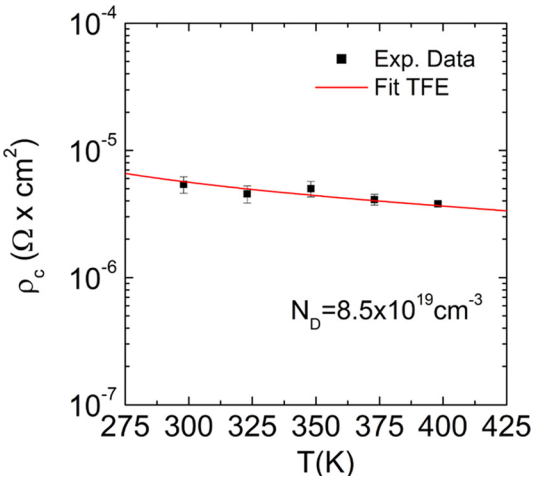

FIG. 4. Specific contact resistance ρ_c of Ni_2Si Ohmic contacts on degenerate n-type implanted 4H-SiC as a function of the measurement temperature T. The continuous line is the thermionic field emission (TFE) fit obtained with $N_D = 8.5 \times 10^{19}$ cm^{-3}.

where q is the electron charge, ε_s is the semiconductor permittivity, h is Planck's constant, and m^* is the effective electron mass.

Considering the electrically active P-concentration determined by the SCM analysis, a value of $E_{00} \approx 90$ meV can be estimated, which, compared with the thermal energy kT at room temperature, gives a ratio $\frac{E_{00}}{kT} \approx 3.6$. Hence, the TFE mechanism is estimated as the dominant mechanism of the current transport in the metal/semiconductor junction.[19,25] Indeed, as can be seen in Fig. 4, the experimental ρ_c data are well described with the TFE model, considering a donor concentration of $N_D = 8.5 \times 10^{19}$ cm^{-3}. This value corresponds to the donor concentration at the recessed metal/4H-SiC interface after the Ni_2Si formation. Noteworthy, this N_D value extrapolated by the TFE fit is in very good agreement with that obtained by the SCM measurement in the plateau region. This latter demonstrates that the silicide formation process did not affect the active P-dopant profile.

In conclusion, active dopant profiling in the degenerate n-type doped 4H-SiC layers, fabricated by high-dose P-implantation (10^{20} atoms/cm^3), has been demonstrated by the combination of the Hall-effect integral carrier density measurement and scanning capacitance microscopy. An electrically active P-dose >80% and a plateau active concentration of (8.5–9) $\times 10^{19}$ cm^{-3} have been estimated from these analyses. The current transport mechanism at Ni_2Si Ohmic contacts fabricated on the degenerate n-type doped 4H-SiC layers was investigated by the temperature-dependent specific contact resistance measurements. In particular, the donor concentration at the Ni_2Si/4H-SiC interface, evaluated by fitting the ρ_c behavior with the thermionic field emission model, was in excellent agreement with the value independently obtained by the SCM depth profiling, also confirming that the current transport in this degenerate doping regime can still be described by the TFE.

The demonstrated active profiling methodology and the insights into the transport mechanisms of Ohmic contacts to degenerate n-type 4H-SiC can have important implications in the 4H-SiC device technology.

The authors would like to acknowledge their colleagues S. Di Franco and D. Corso for their valuable support during the clean room sample processing and Hall-effect measurements.

DATA AVAILABILITY

The data that support the findings of this study are available from the corresponding author upon reasonable request.

REFERENCES

[1]T. Kimoto and J. Cooper, *Fundamentals of Silicon Carbide Technology: Growth, Characterization, Devices and Applications* (John Wiley & Sons, Singapore, 2014).
[2]F. Roccaforte, P. Fiorenza, G. Greco, R. Lo Nigro, F. Giannazzo, A. Patti, and M. Saggio, Phys. Status Solidi A **211**, 2063–2071 (2014).
[3]F. Roccaforte, P. Fiorenza, G. Greco, R. Lo Nigro, F. Giannazzo, F. Iucolano, and M. Saggio, Microelectron. Eng. **187-188**, 66–77 (2018).
[4]J. Wong-Leung, M. S. Janson, A. Kuznetsov, B. G. Svensson, M. K. Linnarsson, A. Hallén, C. Jagadish, and D. J. H. Cockayne, Nucl. Istrum. Methods Phys. Res., Sect. B **266**, 1367–1372 (2008).
[5]S. Contreras, L. Konczewicz, R. Arvinte, H. Peyre1, T. Chassagne, M. Zielinski, and S. Juillaguet, Phys. Status Solidi A **214**, 1600679 (2017).
[6]S. Asada, T. Okuda, T. Kimoto, and J. Suda, Appl. Phys. Express **9**, 041301 (2016).
[7]H. Fujhiara, J. Suda, and T. Kimoto, Jpn. J. Appl. Phys., Part 1 **56**, 070306 (2017).
[8]Y. Negoro, K. Katsumoto, T. Kimoto, and H. Matsunami, J. Appl. Phys. **96**, 224 (2004).
[9]R. Nipoti, A. Nath, S. B. Qadri, Y.-L. Tian, C. Albonetti, A. Carnera, and M. V. Rao, J. Electron. Mater. **41**, 457 (2012).
[10]M. Laube, F. Schmid, G. Pensl, G. Wagner, M. Linnarsson, and M. Maier, J. Appl. Phys. **92**, 549 (2002).
[11]F. Schmid, M. Laube, G. Pensl, G. Wagner, and M. Maier, J. Appl. Phys. **91**, 9182 (2002).
[12]M. A. Capano, R. Santhakumar, R. Venugopal, M. R. Melloch, and J. A. Cooper, J. Electron. Mater. **29**, 210 (2000).
[13]F. Giannazzo, P. Fiorenza, and V. Raineri, "Carrier transport in advanced semiconductor materials," in *Applied Scanning Probe Methods*, edited by B. Bhushan, H. Fuchs, and M. Tomitori (Springer-Verlag, Heidelberg, 2008), Vol. 8–10.
[14]F. Giannazzo, L. Calcagno, V. Raineri, L. Ciampolini, M. Ciappa, and E. Napolitani, Appl. Phys. Lett. **79**, 1211–1213 (2001).
[15]F. Giannazzo, F. Roccaforte, and V. Raineri, Appl. Phys. Lett. **91**, 202104 (2007).
[16]P. Fiorenza, F. Giannazzo, M. Vivona, A. La Magna, and F. Roccaforte, Appl. Phys. Lett. **103**, 153508 (2013).
[17]A. Frazzetto, F. Giannazzo, R. Lo Nigro, V. Raineri, and F. Roccaforte, J. Phys. D **44**, 255302 (2011).
[18]F. Roccaforte, F. La Via, and V. Raineri, Int. J. High Speed Electron. Syst. **15**, 781–820 (2005).
[19]D. K. Schroder, *Semiconductor Material and Device Characterization*, 3rd ed. (John Wiley & Sons Inc., Hoboken, NJ, USA, 2006).
[20]J. F. Ziegler, M. D. Ziegler, and J. B. Biersack, Nucl. Istrum. Methods Phys. Res., Sect. B **268**, 1818–1823 (2010).
[21]M. Spera, D. Corso, S. Di Franco, G. Greco, A. Severino, P. Fiorenza, F. Giannazzo, and F. Roccaforte, Mater. Sci. Semicond. Process. **93**, 274–279 (2019).
[22]F. Roccaforte, A. Frazzetto, G. Greco, F. Giannazzo, P. Fiorenza, R. Lo Nigro, M. Saggio, M. Leszczynski, P. Pristawko, and V. Raineri, Appl. Surf. Sci. **258**, 8324–8333 (2012).
[23]M. Rambach, A. J. Bauer, and H. Ryssel, Mater. Sci. Forum **556-557**, 587–590 (2007).
[24]K. Vasilevskiy, K. Zekentes, and N. Wright, "Processing and characterisation of Ohmic contacts to silicon carbide," in *Advancing Silicon Carbide Electronics Technology*, edited by I. K. Zekentes and K. Vasilevskiy (Materials Research Forum LLC., Millersville, 2018), pp 27–126.
[25]F. A. Padovani and R. Stratton, Solid-State Electron. **9**, 695 (1966).